Institut für Veterinärphysiologie
der Vetsuisse-Fakultät Universität Zürich

Direktor: Prof. Dr. Max Gassmann

Arbeit unter Leitung von Dr. Christina N. Boyle

The role of the area postrema in the anorectic effects of amylin and salmon calcitonin - behavioral and neuronal phenotyping

Inaugural-Dissertation

zur Erlangung der Doktorwürde der
Vetsuisse-Fakultät Universität Zürich

vorgelegt von

Fiona Elektra Brägger

Tierärztin

von Zürich, Schweiz

genehmigt auf Antrag von

Prof. Dr. Thomas A. Lutz, Referent

Prof. Dr. Wolfgang Langhans, Korreferent

Zürich 2014

Table of Contents

Zusammenfassung

Amylin reduziert die Grösse einer Mahlzeit über die Area Postrema (AP) und peripher appliziert führt es zu einer cFos-Expression in AP Neuronen. Ungefähr 50% dieser Neurone sind noradrenerg und scheinen Amylin's anorektische Wirkung zu vermitteln. Salmon calcitonin (sCT) ist ein Amylin Agonist und wirkt stark anorektisch, wobei die vermittelnden Neurone nicht bekannt sind. Männliche Wistar Ratten erhielten eine AP-(APX) oder Schein-Läsion (sham). Mahlzeitenmuster wurden unter ad libitum Bedingungen und nach einer Fastenperiode analysiert. Die Rolle der AP bei der anorektischen Wirkung von sCT im Vergleich zu Amylin wurde bei APX und sham Ratten anhand Fütterungsstudien und der Expression von cFos ermittelt. Der Phänotyp der cFos exprimierenden Neurone wurde mittels Mehrfachfärbung gegen cFos und Dopamin-β-Hydroxylase (DBH) oder Tryptophan Hydroxylase (TPH) untersucht. Um einen Unterschied bei dem glutaminergen Input festzustellen, wurde die VGLUT2 Apposition zu Amylin- und sCT aktivierten Neuronen bestimmt. Ähnlich wie bei Amylin, ist eine intakte AP die Voraussetzung für die anorektische Wirkung von sCT und die Ko-Expression von cFos und DBH war auch ähnlich. Die Ko-Expression von cFos und TPH war jedoch vernachlässigbar klein. Wir konnten keine Unterschiede beim glutaminergen Input finden nach Amylin und sCT Behandlung . Unsere Studie konnte aufzeigen, dass Amylin und sCT ähnliche Neurone aktivieren und diese vorwiegend in der AP liegen.

Summary

Amylin reduces meal size via the area postrema (AP). Peripheral amylin leads to the expression of cFos protein in AP neurons; approximately 50% of these neurons are noradrenergic and appear to mediate amylin's anorectic action. Salmon calcitonin (sCT) is an amylin agonist that potently reduces eating but the neurons involved are unknown.

We compared sCT- and amylin-activated hindbrain pathways and the role of the AP. Male Wistar rats underwent surgical lesion of the AP (APX) or sham surgery. Meal patterns were analyzed under ad libitum and post-deprivation conditions. The role of the AP in mediating sCT's anorectic action was examined in feeding experiments and the cFos expression was compared between surgery groups, and relative to amylin. The phenotype of cFos-expressing neurons was examined by testing for the co-expression of dopamine-β-hydroxylase (DBH) or tryptophan hydroxylase (TPH). By measuring the apposition of VGLUT2-positive boutons, potential glutaminergic input to amylin- and sCT-activated AP neurons was compared. An intact AP was necessary for sCT to reduce eating. Co-expression between cFos activation and DBH after amylin or sCT did not differ markedly. Colocalization of cFos and TPH was minor. Approximately 95% of neurons expressing cFos and DBH after amylin or sCT treatment were apposed to VGLUT2-positive boutons. We suggest that the hindbrain pathways engaged by amylin and sCT share many similarities, including the mediation by AP neurons.

Introduction

Amylin and calcitonin are structurally and functionally related peptides of the calcitonin-like gene peptide superfamily (Wimalawansa, 1997). Amylin and calcitonin share a common core receptor, the calcitonin receptor, which is transformed into a specific amylin receptor by receptor activity modifying proteins (Sexton *et al.*, 1994; Christopoulos *et al.*, 1999; Muff *et al.*, 1999). Amylin is co-secreted with insulin from pancreatic β-cells (Butler *et al.*, 1990; Ogawa *et al.*, 1990) and one physiological response that amylin and calcitonin share is the inhibition of eating (Lutz *et al.*, 2000). While the anorectic action of mammalian calcitonin is relatively weak, fish-derived calcitonin, like salmon calcitonin (sCT), has often been used in pharmacological studies aimed at identifying amylin's mechanism of action (Lutz *et al.*, 2000). In contrast to amylin, sCT displays stronger, irreversible receptor binding, which translates into a more potent, longer-lasting eating-inhibitory response (Riediger *et al.*, 1999; Lutz *et al.*, 2000; Reidelberger *et al.*, 2002).

Strong evidence suggests that the area postrema (AP) is an important brain site mediating amylin's anorectic effect (Lutz, 2012). Lesions of the AP and its amylin receptor population abolish peripheral amylin's eating-inhibitory effects (Lutz *et al.*, 1998; Lutz *et al.*, 2001; Mack *et al.*, 2010). Administration of exogenous peripheral amylin induces a strong cFos response in the AP and in several downstream nuclei, including the nucleus of the solitary tract (NTS; Rowland *et al.*, 1997; Rowland & Richmond, 1999; Barth *et al.*, 2004; Riediger *et al.*, 2004). The neurochemical phenotypes of the neurons mediating amylin's and sCT's inhibitory effect on eating are only partially identified. Approximately 50% of amylin-activated cells expressing cFos protein within the AP were also positive for the specific noradrenergic marker, dopamine-beta-hydroxylase (DBH; Potes *et al.*, 2010). These DBH-positive neurons seem to be functionally relevant, because ablating them with saporin toxin reduced amylin's anorectic action (Potes *et al.*, 2010). It is unknown which neuronal populations are specifically activated by sCT, and whether sCT also activates the same noradrenergic population as amylin.

More generally, ablating the AP not only prevents amylin's anorectic effect but also alters physiological feedback mechanisms that lead to a disruption in meal patterns (Ritter & Edwards, 1984; Stricker *et al.*, 1997). Hence, to further probe the role of the AP in respect to food intake control and meal patterns, we first aimed to analyze meal patterns in our rat model of AP lesions, compared to sham lesioned rats. Our second goal was to determine whether equipotent doses of amylin and sCT activate phenotypically similar neuronal populations in the AP. To this end, we assessed whether the cFos expression colocalizes with markers for catecholaminergic and serotoninergic neurons following amylin or sCT administration. Finally, because glutamatergic transmission may underlie several effects mediated by noradrenergic AP neurons (Stornetta *et al.*, 2002), and because this may be relevant for amylin-induced activation of the AP (Fukuda *et al.*, 2013), we evaluated the apposition of vesicular glutamate transporter-2 (VGLUT2)-positive boutons to neurons co-expressing cFos and DBH in the AP after amylin or sCT.

Materials and Methods

Animals. Male Wistar rats (200-250 g; Charles River, Sulzfeld, Germany) were maintained at a constant ambient temperature (21 ± 1°C) under an artificial 12 h light/dark cycle with food and water available ad libitum, unless noted otherwise. Rats were fed a standard chow diet (no. 3430, Provimi Kliba, Gossau, Switzerland) during the experiments. All experiments were performed with the approval of the Veterinary Office of the Canton Zurich, Switzerland, and in accordance with the EU Directive 2010/63/EU on the protection of animals used for scientific purposes.

Drugs. Salmon calcitonin and amylin (Bachem AG, Bubendorf, Switzerland; catalogue numbers: amylin H-9475.1000, sCT H-2260.0001) were reconstituted with saline and diluted with saline to final doses of 1, 5 or 10 µg/kg, with an injection volume of 1 ml/kg.

Surgery. Rats were anesthetized (IP) using a mixture of ketamine (50 mg/kg, Narketan, Vétoquinol AG, Ittingen, Switzerland), xylazine (2.5 mg/kg, Xylazin, Streuli Pharma AG, Uznach, Switzerland), and acepromazine (0.75 mg/kg, Prequillan, Arovet AG, Dietikon, Switzerland). The head of the rat was flexed ventrally at an approximate 110-degree-angle in a stereotaxic frame. Skin and three layers of neck musculature were cut and retracted for visualization of the foramen magnum. Under visual control with a surgical microscope, the cranial dura mater was penetrated with an angled cannula tip and the CSF was blotted. AP lesions were performed by aspirating the AP with a blunted cannula tip fixed to a flexible tube attached to a vacuum pump (Lutz *et al.*, 1998; Jordi *et al.*, 2013). In sham-lesioned rats, the AP was exposed but not touched. Musculature and skin were sutured respecting the individual muscle layers. Rats received SC injections of 5 ml sterile saline, antibiotics (7.5 mg/kg enrofloxacin, Baytril 2.5%, Provet AG, Lyssach, Switzerland) and an analgesic (1 mg/kg flunixin, Fluniximin, Graeub AG, Bern, Switerland) daily for at least three days post surgery, and were given 1 to 2 weeks to recover from the surgery. At the end of the experiments AP lesions were confirmed

histologically (Lutz *et al.*, 1998; Lutz *et al.*, 2001; Riediger *et al.*, 2004), in parallel with the immunohistochemical quantification.

Experiment 1: Meal pattern analysis in untreated AP-lesioned and sham-lesioned rats. Meal patterns in sham- and AP-lesioned groups (n= 16 and 13, respectively) were analysed using the BioDAQ Food Intake Monitor (Research Diets Inc., New Brunswick, NJ). The technical specifications of the monitoring system have been described previously (Boyle *et al.*, 2011). Rats were habituated to a 12-h fast twice per week followed by 3 days of adaptation to the BioDAQ cages (type 2000P, Tecniplast, Germany). Meal pattern data were collected and analyzed under two conditions. First, eating was recorded for 24h in ad libitum-fed rats. Second, 24-h food intake data were collected after a 12-h fast during the light phase. Meal pattern data collected from each rat were segmented into meals by clustering independent feeding bouts. The criteria defining a meal were a minimum inter-meal interval of 15 min and a minimum meal size of 0.23 g. Data were analyzed using the BioDAQ Monitoring software.

Experiment 2: Behavioral experiments; Dose response study and identification of equipotent eating-inhibitory doses of amylin and sCT. Sham- and AP-lesioned rats were individually housed in hanging wire mesh cages (Indulab AG, Gams, Switzerland, stainless steel, 47x33x20 cm) fitted with external food hoppers. Twice per week, rats were fasted for 12 h during the light phase. Shortly before dark onset rats were injected IP with saline, amylin or sCT; at dark onset, food was given back. Food intake was measured manually using a digital scale after 1, 2, 4 and 24 h. Tests were repeated in a randomized, crossover manner, so that each animal within the surgery group was examined under all conditions. The dose-response relationships for amylin and sCT were assessed using three increasing doses (1, 5, 10 µg/kg). Based on these findings equipotent doses of amylin (10 µg/kg) and sCT (5 µg/kg) were used in a second behavioral experiment.

Experiments 3, 4 and 5: Phenotypic characterization of amylin- and sCT-activated neurons: Rats were fasted for 12 h during the light phase before

receiving injections of saline, amylin (10 µg/kg) or sCT (5 µg/kg) at dark onset. Food was withheld and 90 min later, rats were deeply anesthetized with pentobarbital (100 mg/kg, IP, Cantonal Pharmacy of Zurich, Switzerland), transcardially perfused with 4% paraformaldehyde in 0.1 M phosphate buffer (PB), and brains collected.

Perfused brains were kept in 4% paraformaldehyde for 48 h, followed by cryoprotection in 0.1 M PB (pH: 7.2) containing 20% sucrose for 24 h. Brains where then frozen with hexane (Sigma Aldrich) on dry ice. Six series of 30-µm thick frontal sections (from Bregma -6.36mm to -14.40mm) were cut on a cryostat (Leica microsystems, Wetzlar, Germany). The sections were kept in a cryoprotecting medium (50% 0.1 M PB, 30% ethylene glycol, 20% glycerol) at -20 °C until processing for immunohistochemistry. One series of sections from each brain was processed for the detection of cFos and DBH, one series for the detection of cFos and TPH, and one series was processed for the detection of cFos, DBH and VGLUT2.

Experiment 3: Double staining for cFos and Dopamine-β-Hydroxylase. All rinses were conducted in 0.1 M PB for 10 min. At least four rinses were implemented between every incubation step. Free-floating sections were incubated for 1 hour at room temperature in a blocking solution of 0.1 M PB containing 1% normal donkey or normal goat serum (NDS or NGS) and 0.3% Triton-X (Triton, X-100, Sigma Aldrich, Germany). The primary and secondary antibodies were diluted in 0.1 M PB containing 1% NDS or NGS and 0.3% Triton-X at concentrations described in Table 1. Sections were incubated in the two primary antibody solutions for subsequent overnights (beginning with the cFos antibody) at room temperature, followed by 1-h incubation in fluorochrome-conjugated secondary antibody solutions at room temperature. Stained sections were mounted on gelatinized slides and cover slipped with Citifluor (AF-100, Citifluor LTD, London, UK).

Experiment 4: Double staining for cFos and Tryptophan Hydroxylase. All rinses were conducted in 0.1 M PB for 10 min. At least 4 rinses were implemented between every incubation step. Free-floating sections were

blocked for 1 h at room temperature in 0.1 M PB containing 1% NDS and 0.3% Triton-X (Sigma Aldrich). Sections were incubated overnight at room temperature in the anti-cFos primary antibody diluted in 0.1 M PB, 1% NDS and 0.3% Triton-X. Thereafter, sections were incubated in the corresponding secondary antibody (see Table 1) diluted in 0.1 M PB, 1% NDS and 0.3% Triton-X for 1 h at room temperature. After the incubation with the secondary antibody, the tissue was incubated for 1 h at room temperature in the ABC solution. For visualization of cFos-positive cells, sections were incubated in enhanced 3,3'-diaminobenzidine-tetrahydrochloride (DAB) chromogen solution (0.05% DAB, 0.04% nickel, 0.08% cobalt, and 0.3% H_2O_2 in PBS) for approximately 2 to 5 min. Next, the tissue was incubated in the anti-TPH primary antibody overnight at room temperature and the following day, in the corresponding secondary antibody for 1 h. To visualize TPH-positive cells, a peroxidase substrate system (ImmPACT NovaRED, Vector Laboratories, Burlingame, CA) was used. The sections were incubated in the peroxidase substrate for 2 to 5 min, and then rinsed in distilled water to stop the staining process and wash off the remaining reagents. All concentrations of antibody and chromogen solutions are shown in Table 1. Tissue was mounted on gelatinized slides and left to air dry for up to 1 h. Slides were then dehydrated in an ascending series of clean alcohols, defatted in xylol, and cover slipped with a DPX medium (Fisher Scientific, Reinach, Switzerland).

Quantification and analysis of double immunolabeling. Photomicrographs of all sections containing AP, subpostremal NTS, NTS, dorsal and central raphe nuclei (DR, CR) were taken at 20x magnification and a numeric aperture of 0.5, using a light microscope (Zeiss Imager Z2) fitted with a black and white camera (Zeiss Axiocam HRm) or a color camera (Zeiss Axiocam). cFos-positive cells were counted using ImageJ software (National Institutes of Health, Bethesda, MD). All quantifications were done manually in a blinded manner, counting by eye using the digital images. Sections within the following bregma distances were quantified: -13.56 to -14.40 mm for the AP, -11.76 to – 14.40 mm for the NTS, -6.36 to -9.36 mm for the DR and CR. For each animal, the counts from all sections (corresponding to a particular brain area) were averaged. Final results are reported as group means ± SEM. For

the remainder of this manuscript this method of light microscopical manual counting quantification, will be referred to as LM.

Experiment 5: Triple staining for cFos, Dopamine-β-Hydroxylase and Vesicular Glutamate Transporter-2. Rinses were conducted as above. All incubation and blocking steps were conducted at room temperature. Free-floating sections were first blocked in sequential blocking solutions consisting of 0.1M PB and Avidin (1:10) or Biotin (1:10), for 15 minutes each, followed by blocking in 0.3% Triton-X and 1% NDS in 0.1M PB for 1 hour. Sections were then incubated overnight in a 0.1M PB solution containing 0.3% Triton-X, 1% NDS, and all three primary antibodies (anti-cFos, -DBH and -VGLUT2). On the following day, sections were incubated for 1 hour in a solution of 0.1M PB containing 0.3% Triton-X, 1% NDS and all three fluorochrome-conjugated secondary antibodies (see Table 1). Stained sections were then mounted on gelatinized slides and cover slipped with Citifluor.

Quantification and analysis of triple immunolabeling. All brain sections containing the AP were scanned with a CLSM Leica SP5 Mid UV-VIS confocal microscope equipped with an x-y-z motorized stage and lasers appropriate for detecting Cy3, Alexa 488 and Alexa 647 fluorescence. Scans were taken in the tile mode using a 63x magnification and a numeric aperture (oil immersion) of 1.4. The extent of the AP was marked manually (x/y positions) and the software (LASF, advanced fluorescence lite, 2.6.0, Leica microsystems, Wetzlar, Germany) adjusted the total number of tiles to be scanned. At three randomly chosen x/y coordinates in each section, the thickness of the section was measured manually and then used to define the z-height of all tiles to be scanned at z-increments of 0.5 µm. An overlap of 15% was used for the subsequent stitching of the tiles to generate a complete 3D image of the AP section.

Using the Optical Fractionator (Stereo Investigator 10, MBF Bioscience, Williston, VT; as described previously by West *et al.*, 1991), cFos-positive, DBH-positive, cFos and DBH double-positive cells and VGLUT2 positive boutons were counted using a counting frame size of 80 × 80 µm, a disector

height of 10 µm and a top guard zone of 2 µm. Only VGLUT2-positive boutons that were abutting a neuron's soma were considered. All boutons in apposition to cFos and DBH double-positive cells selected by the Disector probes were counted. Unbiased estimates of the total number of neurons of interest per AP were acquired by multiplying the counts with the inverse of the sampling fractions for sections, area and section thickness. This method of confocal stereological quantification will be referred to as CM for the remainder of this manuscript.

Statistics. Statistical analysis was done using Prism (Graph Pad Software, La Jolla, CA). One-way ANOVA and Student's t- tests were used as appropriate. Bonferroni Post hoc analysis was performed when appropriate. A P-value of <0.05 was considered statistically significant for all experiments.

Experiment 1: T-tests; Sham versus APX within ad-libitum and post-deprivation conditions, n=13-17 per surgery group
Experiment 2: One-way ANOVA; drug as main factor, within surgery (APX or sham) condition, n= 11-13 per surgery group
Experiment 3: One-way ANOVA; drug as main factor, within surgery (APX or sham) condition, n= 13-17 per surgery group
Experiment 4: One-way ANOVA; drug as main factor, within surgery (APX or sham) condition, n= 13-17 per surgery group
Experiment 5: T-tests; amylin 10 µg/kg versus sCT 5 µg/kg within sham-lesioned rats, n= 5-6 per treatment group
Experiment 6: T-tests; comparison of quantitative analysis using CM versus LM within treatment condition (amylin 10 µg/kg or sCT 5 µg/kg), n= 5-6 per treatment group.

Results

Experiment 1: Meal pattern analysis of sham and APX rats

APX rats exhibited altered meal patterns indicative of a change in feedback inhibition of ingestive behavior. Under ad libitum conditions, the size of the first meal was significantly larger in APX than sham rats ($t(26)=5.425$, $p < 0.001$), but APX rats took longer after dark onset to initiate the first meal ($t(26)= 3.028$, $p =0.0055$). Average meal size ($t(26)= 3.870$, $p <0.001$) as well as meal duration ($t(26)= 2.192$, $p= 0.0375$) were significantly increased in APX compared to sham rats. Additionally, sham rats ate more meals per day than APX rats ($t(26)= 3.564$, $p=0.0014$), but the inter-meal interval was not significantly different. Total 24-h food intake did not differ between sham and APX rats as illustrated in Table 2.

In the post-deprivation condition following a 12-hour light phase fast, food intake of APX rats in the following 24 h was significantly reduced compared to sham ($t(26)= 3.128$, $p = 0.0042$). Similar to ad libitum conditions, APX rats consumed significantly fewer meals ($t(26)= 5.728$, $p <0.0001$) and their latency to feed after dark onset was longer ($t(26)= 5.650$, $p <0.0001$). Average meal size, meal duration, size of first meal and the inter-meal interval did not differ significantly between the two surgery groups in this state, which was largely attributed to a deprivation-induced increase in meal size in the sham group that was not observed in the APX group.

Experiment 2.1: Dose response curve

Amylin and sCT dose-dependently decreased eating in sham rats, as previously published (Figure 1A & C; Lutz *et al.*, 2000). Eating was significantly decreased by 5 and 10 µg/kg amylin at the 1-h ($F(3,12) = 7.034$, $p< 0.01$) and by 10 µg/kg amylin at the 2-h time point ($F(3,12) = 5.941$, $p< 0.01$). One µg/kg amylin had no effect on eating and none of the doses decreased eating at the 4-h time point ($F(3,12) = 1.415$, $p> 0.05$). Amylin did not decrease eating in APX rats at any dose or time point (F h-1, -2, -4 $(3,12)= 0.4145$, 0.6527 and 0.9649 respectively, $p> 0.05$ for all; Figure 1B).

Compared to saline and 1 μg/kg, 5 and 10 μg/kg sCT reduced food intake at all times (F h-1, -2, -4, -24 (3,14)= 38.07, 40.16, 67.14 and 401.6 respectively, $p< 0.001$) in sham rats. Five and 10 μg/kg sCT doses were not significantly different from each other. One μg/kg decreased eating only at 4 and 24 h post-injection (F h-4, -24 (3,14)= 67.14 and 401.6 respectively, $p< 0.05$ and $p<0.001$). The AP lesion almost completely blocked the effect of sCT on eating. However, after receiving 5 or 10 μg/kg sCT, 24-h food intake in APX rats was significantly reduced, as shown by a one-way ANOVA and subsequent Bonferroni post-hoc analysis (h-4; $F (3,13) = 3.545$, $p < 0.05$; Figure 1D).

Experiment 2.2: Equipotent doses of amylin and sCT

Figure 2A shows the significant food intake reduction after amylin and sCT in sham rats; in the first hour after injection, 10 μg/kg amylin and 5 μg/kg sCT reduced food intake to a similar extent and there was no significant difference in the eating-inhibitory effect detectable at this time point ($F (2,16) = 13.17$, $p >0.05$). Two and four hours after injection, only sCT but not amylin reduced eating. In the APX rats (Figure 2B) neither peptide evoked a significant reduction of the cumulative food intake in the first two hours. However, there was a significant difference four hours after the injection between sCT and amylin, but not saline controls (one-way repeated-measures ANOVA and Bonferroni post-hoc analysis; $F (2,12) = 7.112$, $p < 0.01$).

Experiment 3:Co-localization of cFos- and DBH- positive neurons in the AP and NTS

One-way ANOVA followed by a Bonferroni post-hoc analysis revealed that 5 μg/kg of sCT produced significantly more cFos-positive cells ($F (2,14) = 122.7$, $p<0.05$) and neurons double-labeled for cFos and DBH than 10μg/kg of amylin ($F (2,14) = 71.7$, $p<0.05$) in the AP (Figure 4A). Relative co-activation was similar, with approximately 44% of the amylin-induced and 47% of the sCT-induced cFos-positive neurons being also positive for DBH; there was no difference between these percentages ($t (5)= 0.7585$, $p=0.4823$). Further, there was no significant difference in number of DBH-positive cells across the treatment groups ($F (2,14) = 1.431$, $P=0.272$; Figure 4A).

Compared to saline, both amylin and sCT treatment resulted in a significant increase in cFos in the NTS of sham rats ($F(2,14) = 12.36$, $p<0.001$; Figure 4B). Amylin (10µg/kg) led to a higher number of double-stained neurons ($F(2,14) = 14.53$, $p<0.05$) and a greater number of DBH-positive cells than sCT (5µg/kg; $F(2,14) = 12.45$, $p<0.01$). Overall, the percentage of colocalization was much lower than in the AP. Neither amylin nor sCT induced cFos expression in the NTS of AP-lesioned rats (Figure 4C). There was no significant difference in the number of DBH-positive cells between the treatment groups ($F= (2,10)=3.357$, $p = 0.0766$).

Experiment 4: Co-localization of cFos- and TPH-positive neurons in hindbrain nuclei

Amylin (10 µg/kg) and sCT (5 µg/kg) significantly increased the number of cFos-positive cells in the AP compared to saline (one-way ANOVA and Bonferroni post-hoc analysis; $F(2, 14) = 67.25$, $p<0.0001$), however no TPH-positive neurons were detected in either group (Figure 5A). Amylin (10 µg/kg) and sCT (5 µg/kg) significantly increased the number of cFos-positive cells in the NTS of sham-lesioned rats ($F(2,14)=18.35$, $p= 0.0001$, n=5-6 per group; Figure 5B). Amylin and sCT treatment did not significantly alter the number of TPH-positive cells in the NTS of sham rats, and there was no appreciable overlap in double-labeled neurons across the three groups. Following APX (Figure 5C), the number of amylin- and sCT-induced cFos-positive cells in the NTS was indistinguishable from saline-treated rats.

One-way ANOVA followed by Bonferroni post-hoc analysis suggested that a constitutive amount of cFos, TPH and a low degree of co-localization (Table 3) of these two markers seemed to be present in the dorsal and central raphe nuclei, independent of treatment and surgery (sham vs. APX).

Experiment 5: Co-localization of cFos- and DBH-positive neurons apposed to VGLUT2-positive boutons in the AP

Using CM, rats treated with sCT exhibited a significantly greater number of cFos-positive cells in the AP, compared to amylin-treated rats ($t(9) = 3.157$, $p = 0.0116$; Figure 6A); this coincides with the results acquired with the standard LM method. Using CM analysis, amylin and sCT did not alter the number of DBH positive cells in the AP ($t(9) = 0.3311$, $p= 0.7482$; Figure 6B). There was a significant difference in the number of double-labeled cells between amylin and sCT ($t(9) = 3.094$, $p= 0.0128$) as shown in Figure 6C, but the percent co-localization did not differ between amylin and sCT. Furthermore, there was no significant difference in the total number of VGLUT2-positive boutons ($t(9) = 2.082$, $p= 0.067$; Figure 6D) or the number of VGLUT2-positive boutons per double-labeled cell ($t(9) = 0.5655$, $p= 0.5855$; Figure 6E) when comparing sCT- and amylin-treated groups. In amylin-treated sham rats, an average of 94.6% of all cells co-expressing cFos and DBH were apposed to VGLUT2-positive boutons, versus a mean of 95.2% for sCT; these percentages did not significantly differ ($t(9) = 0.2411$, $p= 0.8149$).

Based on the Gunderson-Jensen estimator (Gundersen *et al.*, 1999), using a smoothness constant of 1 for the AP, the ratio between mean CE^2 and the observed relative variance CV^2, was less than 0.5 for all the markers estimated, demonstrating that the sampling procedure contributed only little to the observed group variances.

Experiment 6: Comparison of the two methods of quantification

When comparing the results obtained with CM to those obtained with LM, we did not detect a significant difference in the percentage of cFos cells that were double-labeled for cFos and DBH following amylin ($t(5)= 0.1353$, $p= 0.8977$) or sCT treatment ($t(4)= 0.131$, $p= 0.9021$), as depicted in Figure 7A. However, the LM method appeared to underestimate the portion of DBH cells that co-express cFos, compared to CM, in both amylin- ($t(5)= 3.496$, $p= 0.0174$) and sCT-treated groups ($t(4)= 5.703$, $p= 0.0047$; Figure 7B).

Discussion

The AP is a critical brain area for the control of homeostatic nutrient handling. The AP relays information relating to gastric emptying, mediates the formation of conditioned taste aversion, and expresses receptors for many metabolic hormones including amylin, GLP-1, and ghrelin (Edwards *et al.*, 1998; Fry & Ferguson, 2009; Punjabi *et al.*, 2011; Zuger *et al.*, 2013). The purpose of the present study was threefold: First, we characterized meal patterns in sham- and AP-lesioned rats under ad libitum and post-deprivation conditions. Second, we sought to clarify the role of the AP in sCT-induced anorexia over a range of doses, relative to amylin's effect. Finally, we examined and compared the phenotype of hindbrain neurons expressing amylin- and sCT-induced cFos, and thereby used for the first time the CM approach to quantify cells in the AP.

Over the course of our experiments, and consistent with previous work done in our laboratory, it became evident that when using APX rats for behavioral experiments which involved 12-hour fasting, rats did not react the same way as their sham controls. APX rats had a long latency to eat and some didn't start eating for up to 4 hours into the dark phase. Earlier work with AP-lesioned rodents suggested that the AP plays a crucial role in the detection of inhibitory signals triggered by food or fluid ingestion, and that ingestive bouts increase in size after APX because the inhibitory feedback is blunted (Stricker *et al.*, 1997). It has also been proposed that because total daily food intake is similar in control and APX rats, APX disrupts the short-term control of meal pattern but possibly not the long-term control of caloric intake in association with body weight maintenance (Ritter & Edwards, 1984). Consistent with these findings, our analysis of meal patterns showed that although APX and sham rats consumed comparable amounts of chow per day under ad libitum conditions, there were differences in how their meals were structured and how the two groups responded to a 12-hour light phase fast. Under ad libitum conditions, APX ate larger, but fewer meals compared to sham rats. Further, we observed that APX rats ingested a larger first meal after dark-onset than sham rats, but the latency to do so was much longer. After fasting the rats for

12 hours during the light phase, sham rats compensated by eating more food over the subsequent 24-h period than under ad libitum conditions. They did so by increasing their average meal size and reducing the latency to feed after the fast. In contrast, the meal profile in APX rats remained almost unaltered by the metabolic challenge; APX rats consumed even fewer meals than under ad libitum conditions and ate less over the subsequent 24 hours. Hence, APX rats appeared unaffected by the preceding caloric deficit.

It was initially suggested that the disruption in ingestive patterns following AP lesions was a result of the loss of signals of gastric distention (Stricker *et al.*, 1997). Today we know that ablation of the AP not only thwarts a major relay station for vagal and splanchnic sensory information passing from the viscera to the brain, but also destroys several neuronal populations carrying receptors responsive to various hormones controlling food intake. Ablation of AP neurons prevents amylin-induced satiation thus inflating meal size (Lutz *et al.*, 1998; Reidelberger *et al.*, 2002; Potes *et al.*, 2010). The loss of AP neurons carrying GLP-1 receptors (Yamamoto *et al.*, 2003), which likely constitute a neuronal population discrete from amylin-responsive neurons (Zuger *et al.*, 2013), is another potential contributor to the large extended meals observed following APX. The loss of a third receptor population could explain the increased latency to feed under both ad libitum and post-deprivation conditions. Ghrelin receptors are also present in the AP (Zigman *et al.*, 2006) and APX was previously shown to blunt ghrelin's orexigenic effect in rats at least under certain conditions (Gilg & Lutz, 2006). Further, ghrelin exerts a direct effect on the electrical activity of a subpopulation of AP neurons (Fry & Ferguson, 2009). Ghrelin signaling in the AP might be critical for both normal meal initiation and for enhancing food seeking and consumption after a fast. We suggest here that the lack of ghrelin signaling might lead to the delayed initiation to feed in APX rats.

In the second part of our studies, we found that, similar to amylin, an intact AP was necessary to produce sCT's full anorectic action, confirming previous studies (Lutz *et al.*, 2001). Results from the dose-response study showed that at higher doses, sCT is capable of reducing food intake to a certain extent in

APX rats. Thus, while sCT acting on the AP appears to be the primary route of action, we cannot rule out the possibility that sCT may also reduce food intake though an AP-independent mechanism or that some remaining intact AP neurons are sufficient to mediate some reduction in eating after higher doses of sCT. A recent study suggests that the ventral tegmental area (VTA), a key brain center for reward processing, not only expresses all components of the amylin receptor, but also seems to play a role in the direct mediation of the effects of peripheral sCT on food intake (Mietlicki-Baase *et al.*, 2013); it was observed that local VTA administration of an amylin antagonist increased food intake and partly prevented the eating inhibitory effect of peripheral sCT. Therefore, in parallel to the immunohistochemical studies described here, we also analyzed an additional series of tissue sections for the colocalization of the enzyme catalyzing dopamine synthesis, tyrosine hydroxylase (TH) and cFos activation in AP- and sham-lesioned rats treated with either 10 µg/kg of amylin, 5 µg/kg of sCT or vehicle. Although TH-positive neurons were abundant in the VTA of all groups, no cFos was detected under our conditions (unpublished data). These data suggest that further investigation is required to determine the role of the VTA following peripheral treatment with amylin or sCT.

Despite the use of equipotent eating-inhibitory doses, sCT treatment produced a significantly higher number of cFos-positive neurons in the AP than amylin 90 min after injection. However, no difference in cFos was observed at the level of the NTS. APX blocked all NTS cFos activation by both amylin and sCT, further substantiating the importance of the AP for sCT's satiating action and the activation of secondary brain areas. Even when comparing amylin- and sCT-induced activation with the aid of confocal microscopy and stereological techniques—a much more precise method of quantification and visualization of activated neurons—the relative effect was similar. This quantitative difference was likely the result of sCT's ability to bind irreversibly and with higher affinity to amylin binding sites.

In addition to comparing cFos activation after amylin and sCT treatment, we also investigated if sCT recruited additional hindbrain neuronal populations.

We confirmed previously published results from our group using LM and found that approximately 50% of amylin-activated neurons in the AP are noradrenergic (Potes *et al.*, 2010). Consistent with increased cFos expression, a slightly larger total number of sCT-induced cFos neurons co-expressed DBH, compared to amylin. Further, it has been suggested previously that an intact serotonergic system is necessary for calcitonin-induced analgesia (Ormazabal *et al.*, 2001). Because sCT also activates calcitonin receptors, we therefore sought to determine if this system plays a role in other actions, like the suppression of food intake. However, we observed almost no overlap between the expression of cFos and TPH in the AP, NTS, DR or CR. These findings support previous results suggesting that the serotonergic system does not seem to mediate amylin-induced satiation (Lutz *et al.*, 1996; Brunetti *et al.*, 2002), and further demonstrate that activation of these serotonergic neurons is not necessary for sCT to suppress eating.

In the last part of our study, we employed confocal imaging and stereology (CM), to study neuronal activation patterns in the entire AP. Using this method, we determined the apposition of VGLUT2-positive boutons to amylin- and sCT-activated neurons. Further, we used this method to evaluate the co-expression of amylin- and sCT-induced cFos and DBH labeling. A difference in the number of VGLUT2 boutons per activated neuron, which may suggest a difference in the excitatory drive to this population of AP neurons, could potentially underlie the stronger and in particular the longer inhibition of feeding observed after sCT, compared to amylin. However, we found that almost all (~95%) amylin- and sCT-activated neurons were in contact with VGLUT2 boutons, and we did not observe a difference between amylin and sCT in the number of VGLUT2 appositions per double-labeled neuron. These results suggest that, at least following acute treatment, there is no difference in glutamatergic apposition between neurons activated by amylin or sCT. We did not determine if chronic treatment of amylin or sCT would modify the glutamatergic drive of these populations.

The results from our current study underscore the role of the AP in controlling short-term food intake. The meal pattern analysis showed that a lesion of the AP disrupts the negative feedback signals controlling meal size and seems to affect the ability to compensate for an energy deficit following a fast. Further, we found that, like amylin, sCT requires an intact AP to produce its full effect on food intake and to induce cFos in the NTS. We observed that neither peptide induced cFos in TPH-expressing neurons in the NTS, DR, or CR, and detected no difference in the number of VGLUT2 boutons apposed to amylin- or sCT-activated neurons expressing DBH. Use of confocal microscopy confirmed that, like amylin, approximately 50% of sCT-activated neurons in the AP are noradrenergic. The phenotype of the remaining cFos-positive neurons in the AP remains to be defined. Our study demonstrates that the hindbrain mechanisms activated by amylin and its agonist sCT share many similarities; substantial differences, which could be due to an effect of sCT (but not amylin) on calcitonin receptors, were not observed.

References

Barth, S.W., Riediger, T., Lutz, T.A. & Rechkemmer, G. (2004) Peripheral amylin activates circumventricular organs expressing calcitonin receptor a/b subtypes and receptor-activity modifying proteins in the rat. *Brain Res*, **997**, 97-102.

Boyle, C.N., Lorenzen, S.M., Compton, D. & Watts, A.G. (2011) Dehydration-anorexia derives from a reduction in meal size, but not meal number. *Physiology & behavior*.

Brunetti, L., Recinella, L., Orlando, G., Michelotto, B., Di Nisio, C. & Vacca, M. (2002) Effects of ghrelin and amylin on dopamine, norepinephrine and serotonin release in the hypothalamus. *Eur J Pharmacol*, **454**, 189-192.

Butler, P.C., Chou, J., Carter, W.B., Wang, Y.N., Bu, B.H., Chang, D., Chang, J.K. & Rizza, R.A. (1990) Effects of meal ingestion on plasma amylin concentration in NIDDM and nondiabetic humans. *Diabetes*, **39**, 752-756.

Christopoulos, G., Perry, K.J., Morfis, M., Tilakaratne, N., Gao, Y., Fraser, N.J., Main, M.J., Foord, S.M. & Sexton, P.M. (1999) Multiple amylin receptors arise from receptor activity-modifying protein interaction with the calcitonin receptor gene product. *Mol Pharmacol*, **56**, 235-242.

Edwards, G.L., Gedulin, B.R., C., J., Dilts, R.P., C.C., M. & Young, A. (1998) Area postrem (AP)-lesions block the regulation of gastric emptying by amylin. *Neurogastroenterol Motil*, **10**.

Fry, M. & Ferguson, A.V. (2009) Ghrelin modulates electrical activity of area postrema neurons. *Am J Physiol Regul Integr Comp Physiol*, **296**, R485-492.

Fukuda, T., Hirai, Y., Maezawa, H., Kitagawa, Y. & Funahashi, M. (2013) Electrophysiologically identified presynaptic mechanisms underlying amylinergic modulation of area postrema neuronal excitability in rat brain slices. *Brain Res*, **1494**, 9-16.

Gilg, S. & Lutz, T.A. (2006) The orexigenic effect of peripheral ghrelin differs between rats of different age and with different baseline food intake, and it may in part be mediated by the area postrema. *Physiology & behavior*, **87**, 353-359.

Gundersen, H.J., Jensen, E.B., Kieu, K. & Nielsen, J. (1999) The efficiency of systematic sampling in stereology--reconsidered. *J Microsc*, **193**, 199-211.

Jordi, J., Herzog, B., Camargo, S.M., Boyle, C.N., Lutz, T.A. & Verrey, F. (2013) Specific Amino Acids Inhibit Food Intake via the Area Postrema or Vagal Afferents. *J Physiol*.

Lutz, T.A. (2012) Control of energy homeostasis by amylin. *Cell Mol Life Sci*, **69**, 1947-1965.

Lutz, T.A., Del Prete, E., Walzer, B. & Scharrer, E. (1996) The histaminergic, but not the serotoninergic, system mediates amylin's anorectic effect. *Peptides*, **17**, 1317-1322.

Lutz, T.A., Mollet, A., Rushing, P.A., Riediger, T. & Scharrer, E. (2001) The anorectic effect of a chronic peripheral infusion of amylin is abolished in area postrema/nucleus of the solitary tract (AP/NTS) lesioned rats. *Int J Obes Relat Metab Disord*, **25**, 1005-1011.

Lutz, T.A., Senn, M., Althaus, J., Del Prete, E., Ehrensperger, F. & Scharrer, E. (1998) Lesion of the area postrema/nucleus of the solitary tract (AP/NTS) attenuates the anorectic effects of amylin and calcitonin gene-related peptide (CGRP) in rats. *Peptides*, **19**, 309-317.

Lutz, T.A., Tschudy, S., Rushing, P.A. & Scharrer, E. (2000) Amylin receptors mediate the anorectic action of salmon calcitonin (sCT). *Peptides*, **21**, 233-238.

Mack, C.M., Soares, C.J., Wilson, J.K., Athanacio, J.R., Turek, V.F., Trevaskis, J.L., Roth, J.D., Smith, P.A., Gedulin, B., Jodka, C.M., Roland, B.L., Adams, S.H., Lwin, A., Herich, J., Laugero, K.D., Vu, C., Pittner, R., Paterniti, J.R., Jr., Hanley, M., Ghosh, S. & Parkes, D.G. (2010) Davalintide (AC2307), a novel amylin-mimetic peptide: enhanced pharmacological properties over native amylin to reduce food intake and body weight. *Int J Obes (Lond)*, **34**, 385-395.

Mietlicki-Baase, E.G., Rupprecht, L.E., Olivos, D.R., Zimmer, D.J., Alter, M.D., Pierce, R.C., Schmidt, H.D. & Hayes, M.R. (2013) Amylin Receptor Signaling in the Ventral Tegmental Area is Physiologically Relevant for the Control of Food Intake. *Neuropsychopharmacology*.

Muff, R., Buhlmann, N., Fischer, J.A. & Born, W. (1999) An amylin receptor is revealed following co-transfection of a calcitonin receptor with receptor activity modifying proteins-1 or -3. *Endocrinology*, **140**, 2924-2927.

Ogawa, A., Harris, V., McCorkle, S.K., Unger, R.H. & Luskey, K.L. (1990) Amylin secretion from the rat pancreas and its selective loss after streptozotocin treatment. *J Clin Invest*, **85**, 973-976.

Ormazabal, M.J., Goicoechea, C., Sanchez, E. & Martin, M.I. (2001) Salmon calcitonin potentiates the analgesia induced by antidepressants. *Pharmacol Biochem Behav*, **68**, 125-133.

Potes, C.S., Turek, V.F., Cole, R.L., Vu, C., Roland, B.L., Roth, J.D., Riediger, T. & Lutz, T.A. (2010) Noradrenergic neurons of the area postrema mediate amylin's hypophagic action. *Am J Physiol Regul Integr Comp Physiol*, **299**, R623-631.

Punjabi, M., Arnold, M., Geary, N., Langhans, W. & Pacheco-Lopez, G. (2011) Peripheral glucagon-like peptide-1 (GLP-1) and satiation. *Physiology & behavior*, **105**, 71-76.

Reidelberger, R.D., Kelsey, L. & Heimann, D. (2002) Effects of amylin-related peptides on food intake, meal patterns, and gastric emptying in rats. *Am J Physiol Regul Integr Comp Physiol*, **282**, R1395-1404.

Riediger, T., Schmid, H.A., Young, A.A. & Simon, E. (1999) Pharmacological characterisation of amylin-related peptides activating subfornical organ neurones. *Brain Res*, **837**, 161-168.

Riediger, T., Zuend, D., Becskei, C. & Lutz, T.A. (2004) The anorectic hormone amylin contributes to feeding-related changes of neuronal activity in key structures of the gut-brain axis. *Am J Physiol Regul Integr Comp Physiol*, **286**, R114-122.

Ritter, R.C. & Edwards, G.L. (1984) Area postrema lesions cause overconsumption of palatable foods but not calories. *Physiology & behavior*, **32**, 923-927.

Rowland, N.E., Crews, E.C. & Gentry, R.M. (1997) Comparison of Fos induced in rat brain by GLP-1 and amylin. *Regul Pept*, **71**, 171-174.

Rowland, N.E. & Richmond, R.M. (1999) Area postrema and the anorectic actions of dexfenfluramine and amylin. *Brain Res*, **820**, 86-91.

Sexton, P.M., Paxinos, G., Kenney, M.A., Wookey, P.J. & Beaumont, K. (1994) In vitro autoradiographic localization of amylin binding sites in rat brain. *Neuroscience*, **62**, 553-567.

Stornetta, R.L., Sevigny, C.P. & Guyenet, P.G. (2002) Vesicular glutamate transporter DNPI/VGLUT2 mRNA is present in C1 and several other groups of brainstem catecholaminergic neurons. *J Comp Neurol*, **444**, 191-206.

Stricker, E.M., Curtis, K.S., Peacock, K.A. & Smith, J.C. (1997) Rats with area postrema lesions have lengthy eating and drinking bouts when fed ad libitum: implications for feedback inhibition of ingestive behavior. *Behav Neurosci*, **111**, 623-632.

West, M.J., Slomianka, L. & Gundersen, H.J. (1991) Unbiased stereological estimation of the total number of neurons in thesubdivisions of the rat hippocampus using the optical fractionator. *Anat Rec*, **231**, 482-497.

Wimalawansa, S.J. (1997) Amylin, calcitonin gene-related peptide, calcitonin, and adrenomedullin: a peptide superfamily. *Crit Rev Neurobiol*, **11**, 167-239.

Yamamoto, H., Kishi, T., Lee, C.E., Choi, B.J., Fang, H., Hollenberg, A.N., Drucker, D.J. & Elmquist, J.K. (2003) Glucagon-like peptide-1-responsive catecholamine neurons in the area postrema link peripheral glucagon-like peptide-1 with central autonomic control sites. *J Neurosci*, **23**, 2939-2946.

Zigman, J.M., Jones, J.E., Lee, C.E., Saper, C.B. & Elmquist, J.K. (2006) Expression of ghrelin receptor mRNA in the rat and the mouse brain. *J Comp Neurol*, **494**, 528-548.

Zuger, D., Forster, K., Lutz, T.A. & Riediger, T. (2013) Amylin and GLP-1 target different populations of area postrema neurons that are both modulated by nutrient stimuli. *Physiology & behavior*, **112-113**, 61-69.

Table 1. Immunohistochemical reagents

Reagents	Antigen/ conjugate	Host	Type	Source	Catalog no.	Dilution
Primary	cFos	Rb	polyclonal	Calbiochem	PC38	1:10000
Secondary	Anti-rabbit IgG	Dk	Cy3-labeled	Jackson	711-165-152	1:400
Secondary	Anti-rabbit IgG	Dk	Biotinylated	Jackson	711-065-152	1:400
Primary	DBH	Ms	monoclonal	Millipore	MAB308	1:1000
Secondary	Anti-mouse IgG	Dk	Alexa488-labeled	Jackson	715-545-150	1:400
Primary	TPH	Sh	polyclonal	Millipore	AB1541	1:5000
Secondary	Anti-sheep IgG	Dk	Biotinylated	Jackson	713-065-003	1:400
Primary	VGLUT2	Gp	polyclonal	Millipore	AB5907	1:2000
Secondary	Anti-guinea pig	Dk	Alexa647-labeled	Jackson	706-605-148	1:400
Immune-peroxidase	ABC system		Vectastain Elite ABC kit	Vector	PK-6100	1:400
Chromagen	DAB			Sigma	D5637	1:20
Peroxidase Substrate	ImmPact NovaRed			Vector	SK4805	

Table 2. Mean ± SEM meal parameters measured in sham and APX rats under ad libitum conditions and following a 12-h light phase fast

	Ad libitum			Post-deprivation		
	SHAM Mean ± SEM	APX Mean ± SEM	P values	SHAM Mean ± SEM	APX Mean ± SEM	P values
Total food intake/24 h (g)	28.0 ± 0.7	28.1 ± 1.8	0.9438	31.4 ± 1	23.2 ± 2.7	0.0042
Total meal number/24 h	8.0 ± 0.4	5.9 ± 0.5	0.0014	7.7 ± 0.4	4.6 ± 0.3	<0.0001
Average meal size (g)	3.6 ± 0.2	5.0 ± 0.3	0.0007	4.3 ± 0.3	5.4 ± 0.5	0.0537
Meal duration (min)	30.6 ± 2.9	41.5 ± 4.3	0.0375	37.2 ± 4.5	44.9 ± 4.2	0.2360
First meal size (g)	2.7 ± 0.2	5.4 ± 0.5	<0.001	5.5 ± 0.7	5.2 ± 0.5	0.7456
Inter-meal interval (min)	65.8 ± 5.3	60.9 ± 6.9	0.5785	75.1 ± 6.1	82.3 ± 20.8	0.7099
Latency to feed (min)	10.3 ± 3.9	47.7 ± 13.3	0.0055	1.2 ± 0.3	60.6 ± 12.2	<0.0001

Table 3. Mean ± SEM number of cFos-positive, TPH-positive, and double-labeled cells in the Dorsal and Central Raphe nuclei of sham and APX rats after treatment with vehicle, amylin (10 µg/kg) or sCT (5 µg/kg).

Dorsal Raphe nucleus	SHAM			APX		
	Vehicle Mean ± SEM	Amylin 10 µg/kg Mean ± SEM	sCT 5 µg/kg Mean ± SEM	Vehicle Mean ± SEM	Amylin 10 µg/kg Mean ± SEM	sCT 5 µg/kg Mean ± SEM
cFos-positive	9.6 ± 4.3	20.3 ± 5.2	7.2 ± 2.4	6.5 ± 2.5	19.6 ± 6.6	12.0 ± 7.4
Double labeled (cFos+TPH)	2.4 ± 1.3	8.2 ± 3.0	1.8 ± 0.6	0.9 ± 0.5	4.9 ± 2.4	4.5 ± 3.1
TPH-positive	100.6 ± 5.7	117.7 ± 12.1	114.6 ± 22.7	116.4 ± 13.6	109.0 ± 13.2	101.9 ± 13.1

Central Raphe nucleus	SHAM			APX		
	Vehicle Mean ± SEM	Amylin 10 µg/kg Mean ± SEM	sCT 5 µg/kg Mean ± SEM	Vehicle Mean ± SEM	Amylin 10 µg/kg Mean ± SEM	sCT 5 µg/kg Mean ± SEM
cFos-positive	4.4 ± 2.4	8.1 ± 3.0	3.5 ± 1.2	4.0 ± 1.8	10.7 ± 4.7	7.5 ± 3.0
Double labeled (cFos+TPH)	1.1 ± 0.7	2.4 ± 0.8	1.6 ± 0.8	0.4 ± 0.1	2.5 ± 1.2	1.1 ± 0.6
TPH-positive	49.6 ± 7.5	57.1 ± 3.9	53.6 ± 5.7	49.6 ± 2.9	54.9 ± 1.8	49.7 ± 3.7

Figure legends

Figure 1. Amylin and sCT lead to a dose-dependent reduction in cumulative food intake; sCT's effect was more potent and longer lasting.
Mean ± SEM cumulative food intake 1, 2, 4, and 24 hours after injection of vehicle, amylin (1, 5, or 10 μg/kg; A, B) or sCT (1, 5, or 10 μg/kg; C, D) in sham-lesioned (A, C) and APX rats (B, D). * significantly different from vehicle $p \leq 0.05$, ** $p \leq 0.01$, *** $p \leq 0.001$; °°° significantly different from amylin (1 μg/kg) $p \leq 0.001$

Figure 2. Amylin (10 μg/kg) and sCT (5 μg/kg) reduced cumulative food intake similarly in sham rats in the first hour after injection compared to vehicle. Neither amylin nor sCT reduced eating in APX rats compared to the respective control.
Mean ± SEM cumulative food intake 1, 2, and 4 hours after injection of vehicle, amylin (10 μg/kg) or sCT (5 μg/kg) in sham-lesioned (A) and APX rats (B). ** significantly different from vehicle $p \leq 0.01$, *** $p \leq 0.001$; °° significantly different from amylin (10 μg/kg) $p \leq 0.01$

Figure 3. Representative images showing co-localization of cFos- (red nuclei) and DBH- expressing (green cell bodies) neurons in the AP of sham rats after (A) saline, (B) amylin (10 μg/kg), (C) sCT (5 μg/kg) treatment. Representative images showing minimal co-localization of cFos- (black nuclei) and TPH-expressing (orange cell bodies) neurons in the dorsal raphe nucleus of sham (D) and APX (E) rats treated with 5 μg/kg of sCT. Representative images showing the co-localization of cFos (red nuclei), DBH (green cell bodies), and VGLUT2 (cyan boutons) in the AP of sham rats treated with 10 μg/kg amylin (F) or 5 μg/kg of sCT (G). High-magnification confocal scan of AP from sham rat treated with 5 μg/kg of sCT showing example of VGLUT2 bouton (white arrow) apposed to a neuron co-expressing cFos and DBH (H).

Figure 4. Amylin and sCT-induced cFos co-localizes with DBH-positive neurons in the AP and NTS of sham rats.
Mean ± SEM number of cFos-positive, DBH-positive, and double-labeled cells in the AP (A) and NTS (B) of sham rats, and the NTS of APX rats (C) after treatment with vehicle, amylin (10 μg/kg) or sCT (5 μg/kg). ** significantly different from vehicle $p \leq 0.01$, *** $p \leq 0.001$; ° significantly different from amylin (10 μg/kg) $p \leq 0.05$

Figure 5. Amylin and sCT-induced cFos does not co-localize with TPH-positive neurons in the AP and NTS of sham rats.
Mean ± SEM number of cFos-positive, TPH-positive, and double-labeled cells in the AP (A) and NTS (B) of sham rats, and the NTS of APX rats (C) after treatment with vehicle, amylin (10 μg/kg) or sCT 5 (5 μg/kg). ** significantly different from vehicle $p \leq 0.01$, *** $p \leq 0.001$

Figure 6. Using CM, approximately 50% of cFos-positive cells were also DBH-positive after amylin (10 µg/kg) and sCT (5 µg/kg) and there was a similar apposition of VGLUT2-positive boutons in amylin- (10 µg/kg) and sCT- (5 µg/kg) treated sham rats.
Mean ± SEM unbiased estimation of the number of cFos positive cells (A), DBH-positive cells (B) and cFos and DBH double-labeled cells (C) in the entire AP of sham rats treated with 10 µg/kg amylin or 5 µg/kg sCT, as quantified using the CM method. Mean ± SEM unbiased estimation of the total number of VGLUT2-positive boutons apposed to neurons co-expressing cFos and DBH (D) and average number of VGLUT2 positive boutons per double-labeled cell (E) in the entire AP of sham rats treated with 10 µg/kg amylin or 5 µg/kg sCT. + significantly different from amylin (10 µg/kg) $p \leq 0.05$

Figure 7. Compared to CM, LM underestimated the degree of DBH-expressing neurons that also express cFos, but not cFos-expressing neurons that also express DBH. Mean ± SEM percentage of total cFos-positive cells that co-localize with DBH (A) and the percentage of total DBH-positive cells that co-localize with cFos (B) in the AP of sham rats treated with 10 µg/kg amylin or 5 µg/kg sCT, as calculated using LM (light microscopical manual counting quantification) and CM (confocal stereological quantification) methods of quantification. * significantly different from LM $p \leq 0.05$, ** $p \leq 0.01$

Figure 1.

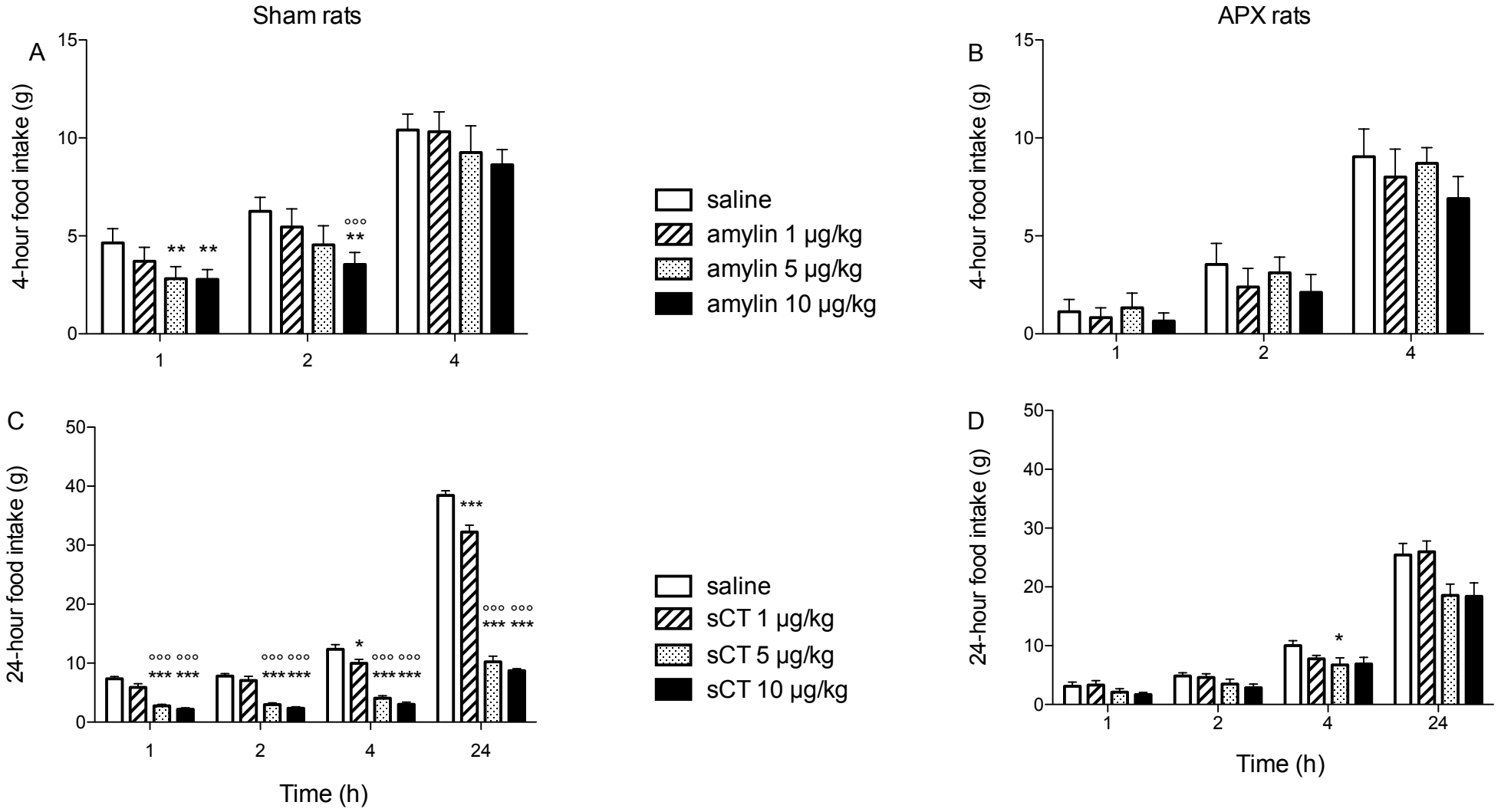
Sham rats
APX rats
A
B
C
D
4-hour food intake (g)
24-hour food intake (g)
Time (h)
saline
amylin 1 µg/kg
amylin 5 µg/kg
amylin 10 µg/kg
sCT 1 µg/kg
sCT 5 µg/kg
sCT 10 µg/kg

Figure 2.

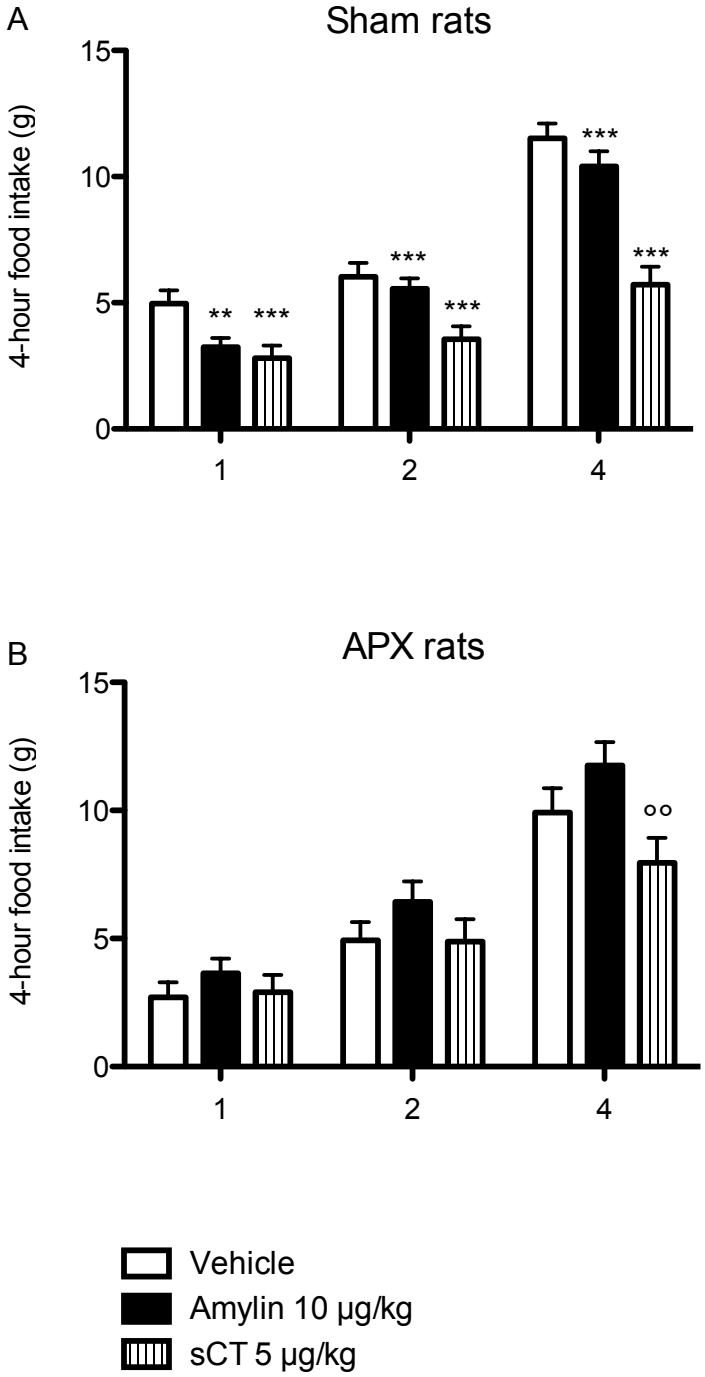
A
Sham rats
4-hour food intake (g)
15
10
5
0
**
***
***
***
***
1
2
4
B
APX rats
4-hour food intake (g)
15
10
5
0
oo
1
2
4
Vehicle
Amylin 10 µg/kg
sCT 5 µg/kg

Figure 3.

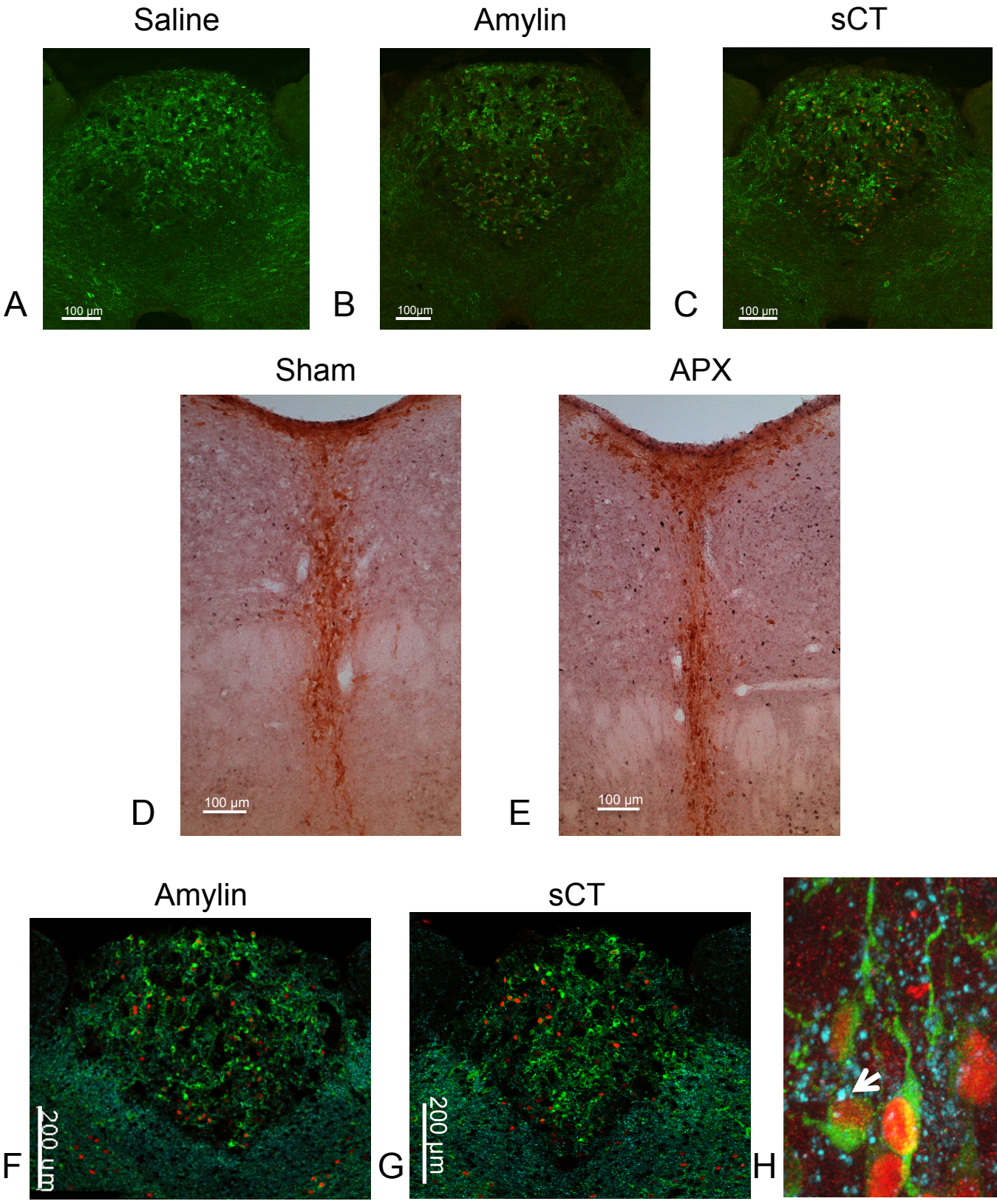
Saline
Amylin
sCT
A
100 µm
B
100µm
C
100 µm
Sham
APX
D
100 µm
E
100 µm
Amylin
sCT
F
200 µm
G
200 µm
H

Figure 4.

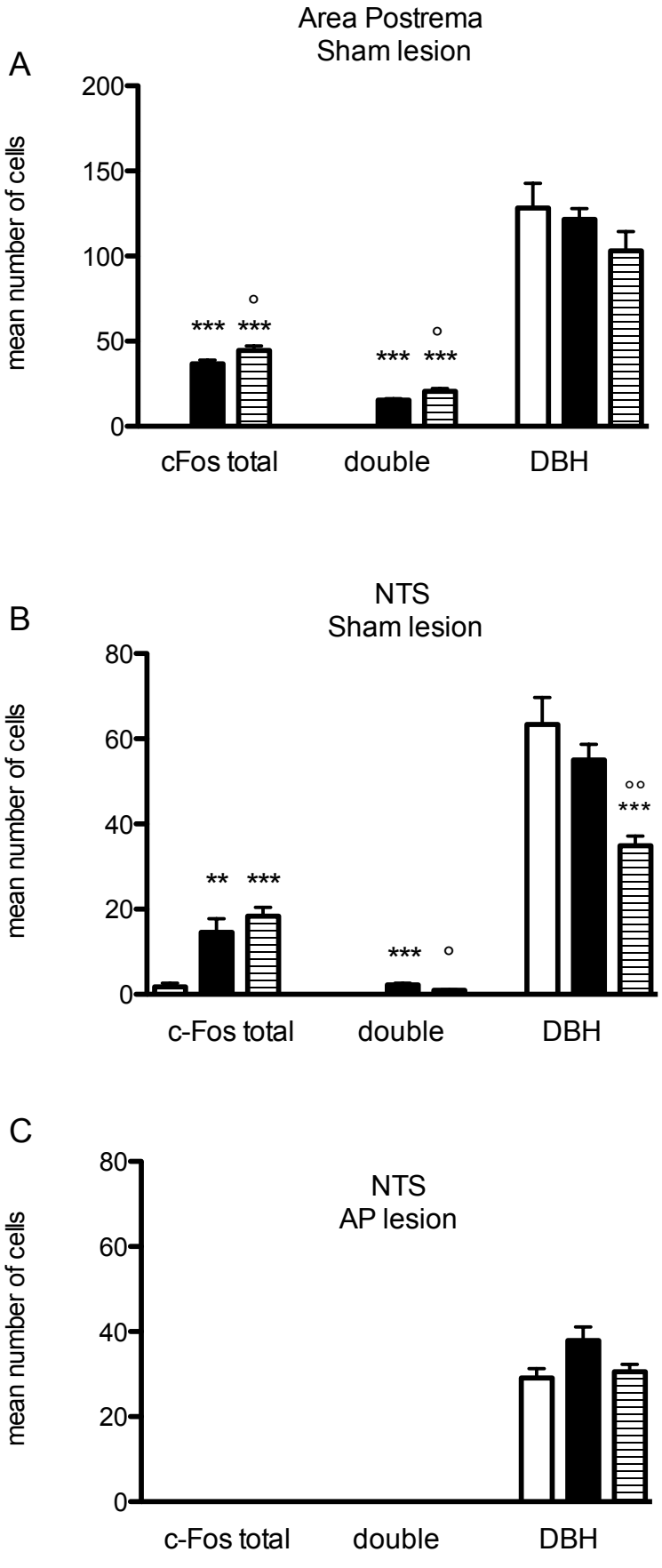
A
Area Postrema
Sham lesion
mean number of cells
200
150
100
50
0
*** ***
°
*** ***
°
cFos total
double
DBH
B
NTS
Sham lesion
mean number of cells
80
60
40
20
0
** ***
*** °
°°
***
c-Fos total
double
DBH
C
NTS
AP lesion
mean number of cells
80
60
40
20
0
c-Fos total
double
DBH
Vehicle
Amylin 10 µg/kg
sCT 5 µg/kg

Figure 5.

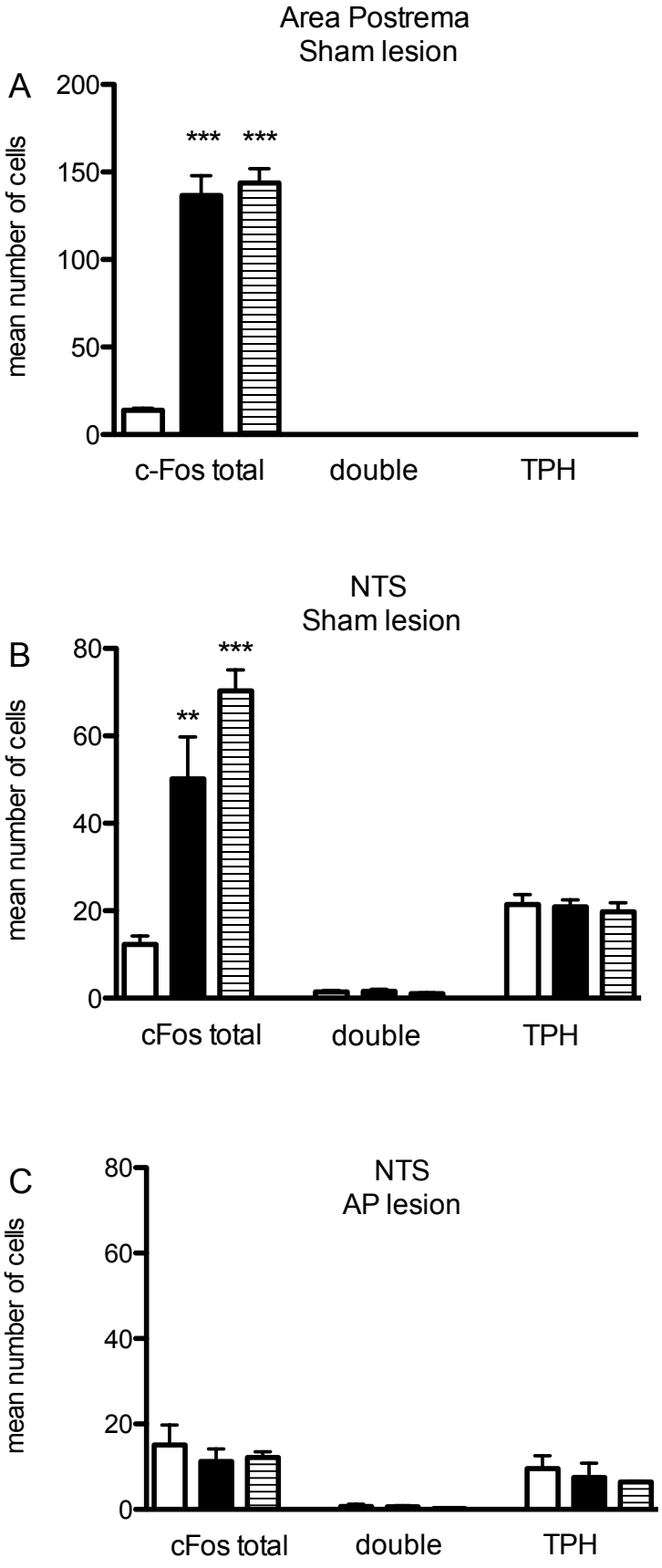
A
Area Postrema
Sham lesion
mean number of cells
200
150
100
50
0
***
***
c-Fos total
double
TPH
B
NTS
Sham lesion
mean number of cells
80
60
40
20
0
**
***
cFos total
double
TPH
C
NTS
AP lesion
mean number of cells
80
60
40
20
0
cFos total
double
TPH
Vehicle
Amylin 10 µg/kg
sCT 5 µg/kg

Figure 6.

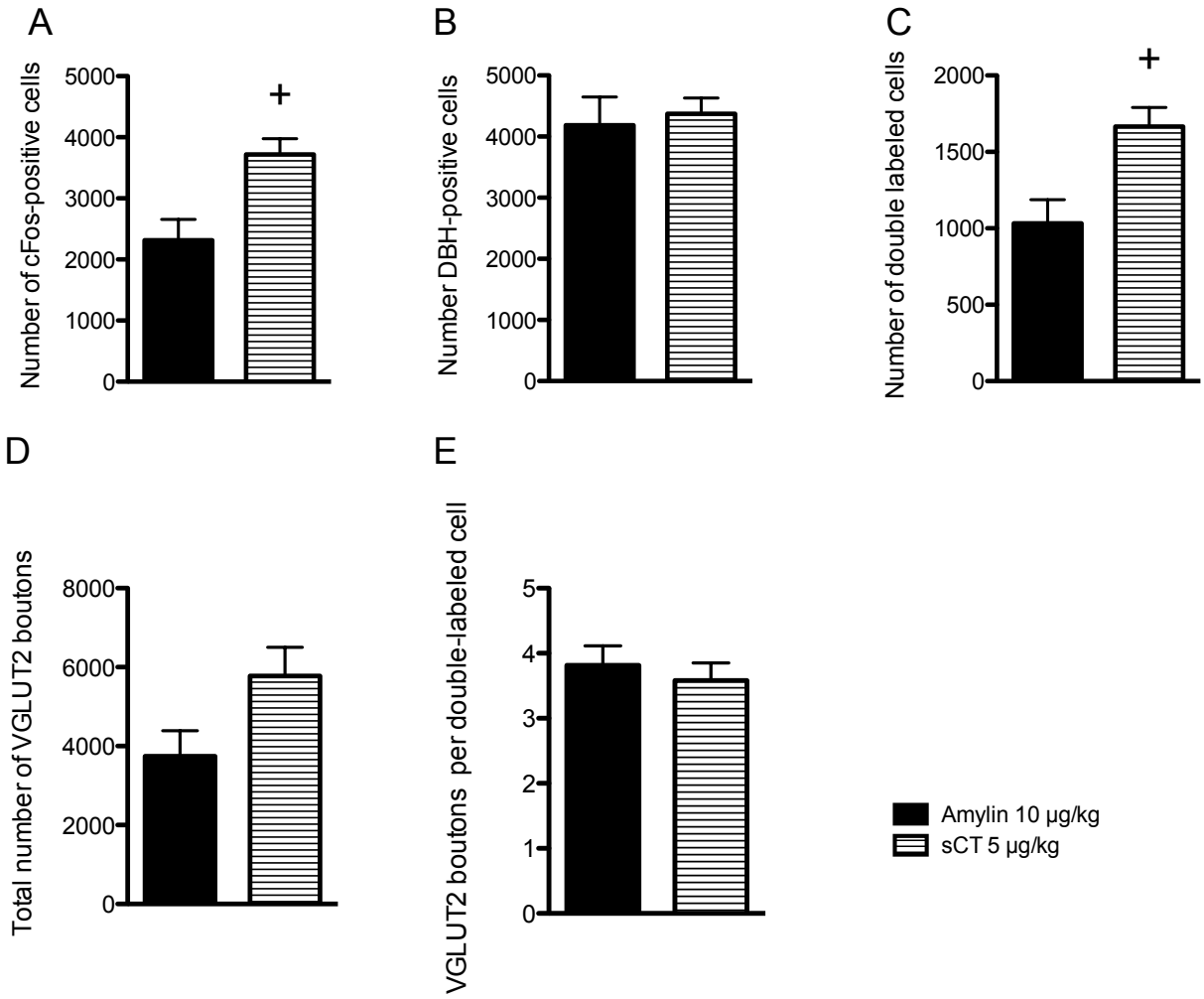
A
Number of cFos-positive cells
5000
4000
3000
2000
1000
0
+
B
Number DBH-positive cells
5000
4000
3000
2000
1000
0
C
Number of double labeled cells
2000
1500
1000
500
0
+
D
Total number of VGLUT2 boutons
8000
6000
4000
2000
0
E
VGLUT2 boutons per double-labeled cell
5
4
3
2
1
0
Amylin 10 µg/kg
sCT 5 µg/kg

Figure 7.

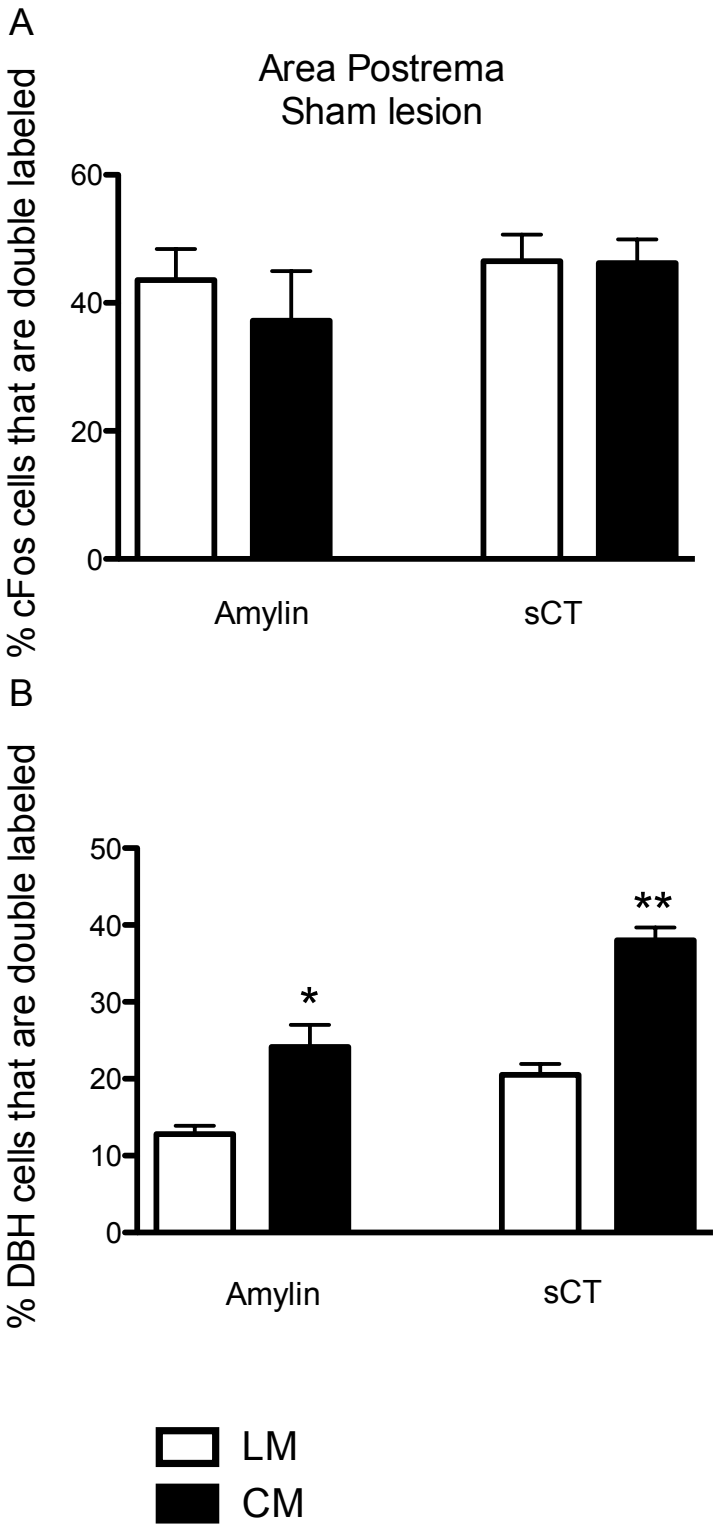
A
Area Postrema
Sham lesion
% cFos cells that are double labeled
60
40
20
0
Amylin
sCT
B
% DBH cells that are double labeled
50
40
30
20
10
0
*
**
Amylin
sCT
LM
CM

List of Abbreviations

AP	Area postrema
APX	Area postrema lesion/lesioned
CM	Confocal stereological quantification method
CR	Central raphe nucleus
DBH	Dopamine-beta-hydroxylase
DR	Dorsal raphe nucleus
LM	Light microscopical manual counting method
NDS	Normal donkey serum
NGS	Normal goat serum
NTS	Nucleus of the solitary tract
PB	Phosphate buffer
sCT	Salmon calcitonin
TPH	Tryptophan-hydroxylase
VGLUT2	Vesicular glutamate transporter 2
VTA	Ventral tegmental area

Acknowledgements

This work was supported by Novo Nordisk and the Swiss National Science Foundation. We gratefully acknowledge the technical guidance and assistance of Dr. Lutz Slomianka, Dr. Kathrin Abegg, and Dr. Urs Ziegler. Imaging was performed with support of the Center for Microscopy and Image Analysis, University of Zurich.

I would like to thank:

Thomas Lutz for giving me the opportunity to write this manuscript

Christina N. Boyle for her steadfast supervision, boundless help and major support throughout the whole affair!

Annika for the help with the laborious experiments in the NGZ

Kathrin for statistics and other interesting discussions

Lori for all the help with the stainings and other questions and problems that occurred…

Everybody else at the institute who contributed to a great working atmosphere or helped me with my experiments!

The ZMB Irchel, especially Urs Ziegler for the great pictures

Lutz Slomianka for the unlimited support and help with the analysis

Martin and my family